Rev. Roum. Sci. Techn.– Électrotechn. et Énerg.
Vol. **69**, *3*, pp. 311–316, Bucarest, 2024

ANALYSIS OF BIDIRECTIONAL DC-DC POWER CONVERTERS FOR SCREENING SYSTEMS OF RETIRED BATTERIES

TEODOR-IULIAN VOICILA[1], GEORGE-CALIN SERITAN[1], BOGDAN-ADRIAN ENACHE[1,*]

Keywords: Bidirectional DC-DC power converters; Screening system; Retired batteries.

With the rapid expansion of energy storage technologies, the concept of the second-life battery has become a central element in sustainability and energy efficiency efforts. This innovative approach refers to the further use of batteries, which have reached the end of life, integrating them into applications with lower energy requirements than those in the automotive industry. The batteries must first be evaluated using a screening system that contains a power converter to apply different test profiles and a measurement and control circuit. This article outlines key performance considerations of bidirectional DC-DC power converter topologies and compares them using multi-criteria analysis to determine which design is more suitable for screening systems. The chosen power converters are further studied in the LTspice program for a detailed comparison based on the obtained results.

1. INTRODUCTION

The increasing adoption of electric and hybrid vehicles highlights concerns regarding pollution and public health [1–4]. Industry forecasts predict a significant global market share for electric vehicles [5, 6]. To address sustainability issues and extend operational lifetimes, the second use of electric vehicle batteries is a promising solution [7, 8]. Accurate performance evaluation of these batteries is crucial for successful integration into less-demanding second-life applications.

A comprehensive screening system must ensure optimal energy provision, charge/discharge rate control, and failsafe operation during malfunctions [9, 10]. Battery performance depends on usage history, as electrochemical processes during charge/discharge cycles can lead to degradation or failure [11]. For instance, excessive charging currents can induce rapid temperature increases, negatively impacting battery longevity.

An intelligent testing system comprises monitoring, control, and power conversion units. The system dynamically determines an optimal testing profile based on battery chemistry and current condition, ensuring safe operation and compliance with relevant standards [12, 13]. With the growing rechargeable battery market, demands on testing systems are intensifying, encompassing efficiency, reduced operational time, extended battery lifespan, autonomous strategy selection, precise parameter monitoring, reliability, affordability, compactness, and a user-friendly interface [14–16]. Consequently, choosing DC-DC conversion topology within the testing circuit is paramount.

DC-DC power converters facilitate battery charging by mediating the conversion and storage of electrical energy as chemical energy. These devices often incorporate linear regulators or switching converters to adjust voltage and current according to the specific battery chemistry. Careful design aligns with application requirements and battery specifications. The power converter directly influences energy efficiency and system flexibility by enabling changes in current and voltage polarity. The proposed system leverages this bidirectional capability to test two or more batteries simultaneously.

The principal contributions of this paper are delineated as follows:

- An analysis of the technical characteristics of bidirectional DC-DC power converter topologies (section 2);
- A comparative study of bidirectional DC-DC power converter topologies employing a multi-criteria analysis approach (section 3);
- The validation of results through simulations in LTspice considering four operational scenarios (section 4).

2. MATERIALS AND METHOD

Considering the many criteria and diverse options available for each criterion within the comparative analysis delineated in Table 2, selecting an appropriate topology for a given application becomes markedly complex. Consequently, to derive a singular conclusion from this evaluation or to generate multiple conclusions that are specifically adapted to the application's structure, the methodology of multi-criteria analysis (MCA) will be employed. This analytical technique facilitates the structured and concurrent consideration of numerous criteria to inform decision-making in complex scenarios. For each criterion, a scoring range from 0 to 100 will be allocated, with 100 denoting the most favorable scenario and 0 representing the least favorable. After establishing a matrix populated with these scores, as depicted in Table 3, a performance matrix will be constructed, shown in Table 4. Within this matrix, each criterion is assigned a weight, articulated as a percentage, ensuring that the aggregate weight equals 100 %. The distribution of weights is as follows: operational type is allocated 15%, the number of inductors/transformers 10 %, the number of capacitors 10%, the number of switches 5 %, the number of diodes 5 %, power density 15 %, complexity 10 %, dimensions 10 %, cost 5 %, and efficiency 15 %. The total of these weights reaches the maximum of 100%. This weighting scheme aligns with the methodology established in [17].

Figure 1 illustrates the cascaded buck-boost converter's power circuit. Control is realized through voltage sources replicating PWM signals for output voltage regulation.

Removing switches S3 and S4 and adjusting the output capacitor value yields the Buck-Boost bidirectional DC-DC converter, as presented in Fig. 2. The difference between the two topologies is that the Buck-Boost type converter can step down the voltage in one direction and step up the voltage in the other. In contrast, cascaded buck-boost can step down and step up voltage in both directions.

Circuit behaviors are simulated in LTspice XVII, a robust SPICE software designed for accurate analog and integrated circuit modeling. Following the design stage, components are selected, and their macro-models and specifications are implemented (Table 1).

[1] National University of Science and Technology "Politehnica" Bucharest, Department of Measurements, Electrical Apparatus and Static Converters, Bucharest, Romania
Emails: iulian.voicila@upb.ro, george.seritan@upb.ro, bogdan.enache2207@upb.ro (correspondence)

DOI: 10.59277/RRST-EE.2024.69.3.10

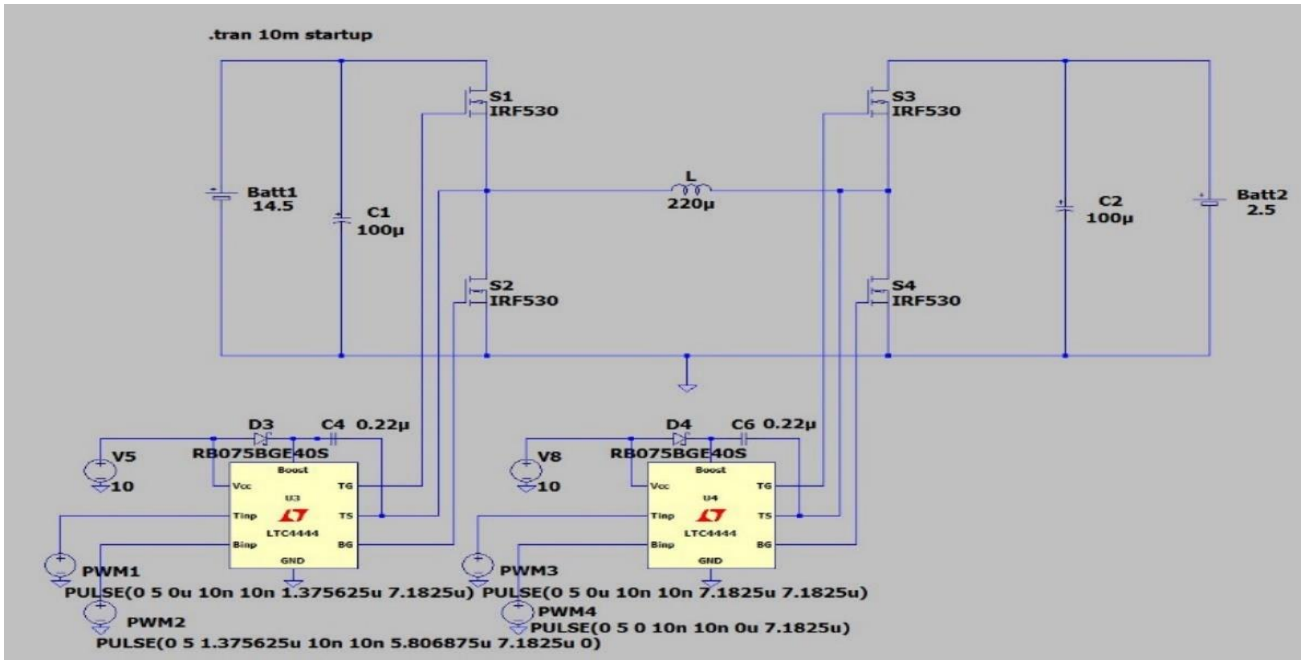

Fig. 1 – Circuit diagram of the bidirectional DC-DC cascaded buck-boost power converter.

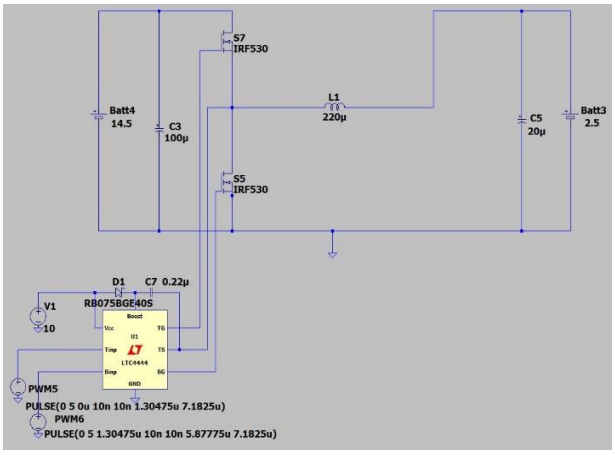

Fig. 2 – Circuit diagram of the bidirectional DC-DC buck-boost power converter

Table 1
Technical specifications of the circuit elements

Circuit element	Name of the component	Supplier	Technical characteristics
Inductor	744375292 03221	Wurth Elektronik	L = 220±20 % µH DCR = 36.45 mΩ IL = 8.8 A Isat = 14.1 A
Capacitor Cascaded Buck-Boost	875115655 003	Wurth Elektronik	C = 100±20 % µF VmaxC = 35 V ESR = 30 mΩ
Capacitor Buck-Boost	875115655 003	Wurth Elektronik	C = 20±20 % µF VmaxC = 35 V ESR = 30 mΩ
Power switch	IRF530SPB F	Vishay	V_DS = 100 V ISmax = 14 A Pd = 88 W RDS = 0.16 Ω
Power driver	LTC4444	Linear Technology	VCC = 7.2-13.5 V VIN = 0-100 V Imax = 2.5 A
Driver capacitor	T499A224 K035ATE1 8K	Kemet	C = 0.22±10 % µF VmaxC = 35 V ESR = 18 mΩ
Driver diode	RB075BGE 40S	Rohm	VRRM = 40 V IAVG = 5 A

The cascaded buck-boost converter's output capacitor is five times larger than the Buck-Boost topology. Design parameters include 14.5V input voltage, 2.5 V output voltage, 128 kHz switching frequency, 1A maximum output current, 10 % current ripple, and 5 % voltage ripple.

3. COMPARATIVE STUDY OF BIDIRECTIONAL DC-DC POWER CONVERTERS

Prior research has comparatively analyzed bidirectional DC-DC topologies, both isolated and non-isolated. In [18], the authors conducted a comparative analysis of non-isolated and isolated bidirectional converter topologies, presenting six non-isolated and two isolated converters alongside their respective advantages and disadvantages. However, this study provides a broad overview without delving into specific applications. A parallel investigation is documented in [19], where the classification and comparative analysis of isolated versus non-isolated converters are outlined, yet it needs a detailed comparison among the topologies. Lithesh et al. offered a more granular classification of bidirectional DC-DC converters [20]. This classification encompasses an explanation and evaluation of each topology according to five distinct criteria: the number of switches, the number of inductors/transformers, the number of capacitors, gain ratio, and efficiency. The study culminates in a synthesized overview of bidirectional DC-DC converters, rating features such as demerits, efficiency, power density, complexity, and gain ratio on a scale from "low" to "high" to facilitate comparison. Despite the breadth of this analysis, it broadly outlines a methodology for selecting the optimal topology. Still, it falls short of addressing the specific requirements for selecting a bidirectional DC-DC power converter for energy transfer among two or more batteries. Hence, this paper endeavors to compare known power converter topologies based on a set of criteria.

Table 2

Comparative study of bidirectional DC-DC power converters [18], [20–28]

Type of electrical insulation	Topology	Operating type	No. of L/T	No. of C	No. of SW	No. of D	Power density	Complexity	Dimension	Cost	Efficiency
Uninsulated	Buck-Boost	2Q	1	2	2	2	Low	Low	Low	Low	> 90 %
	Cuk	2Q	2	3	2	2	Medium	Low	Medium	High	>92 %
	SEPIC-Zeta	2Q	2	3	2	2	Medium	Low	Medium	High	>94 %
	Cascaded Buck-Boost	4Q	1	2	4	4	High	Medium	Medium	Medium	>94 %
	Switched Capacitor	2Q	0	3	4	4	High	Medium	High	Medium	>88 %
	Interleaved	2Q	2	2	4	4	Low	Medium	High	High	>94 %
Insulated	Flyback	2Q	1	2	2	2	Medium	Low	Medium	High	>82 %
	Dual H-bridge	2Q	1/1	5	4	4	Medium	Medium	Very high	Very high	>92 %
	Dual active bridge	4Q	1/1	2	8	8	High	High	Very High	Very high	>93 %
	Push-Pull	2Q	1/1	2	4	4	Medium	Medium	High	High	>86 %
	Forward	2Q	1/1	2	2	2	Medium	Low	Medium	High	>88 %

Table 3

Score matrix

Type of electrical insulation	Topology	Operating type	No. of L/T	No. of C	No. of SW	No. of D	Power density	Complexity	Dimension	Cost	Efficiency
Uninsulated	Buck-Boost	66.7	75	100	100	100	33.3	100	100	100	95.74
	Cuk	66.7	50	66.7	100	100	66.7	100	75	50	97.87
	SEPIC-Zeta	66.7	50	66.7	100	100	66.7	100	75	50	100
	Cascaded Buck-Boost	100	75	100	66.7	66.7	100	66.7	75	75	100
	Switched Capacitor	66.7	100	66.7	66.7	66.7	100	66.7	50	75	93.61
	Interleaved	66.7	50	100	66.7	66.7	33.3	66.7	50	50	100
Insulated	Flyback	66.7	75	100	100	100	66.7	100	75	50	87.23
	Dual H-bridge	66.7	25	33.3	66.7	66.7	66.7	66.7	25	25	97.87
	Dual active bridge	100	25	100	33.3	33.3	100	33.3	25	25	98.93
	Push-Pull	66.7	25	100	66.7	66.7	66.7	66.7	50	50	91.48
	Forward	66.7	25	100	100	100	66.7	100	75	50	93.61

Table 4

Performance matrix

Type of electrical insulation	Topology	Operating type	No. of L/T	No. of C	No. of SW	No. of D	Power density	Complexity	Dimension	Cost	Efficiency	Total [%]
Uninsulated	Buck-Boost	10	7.5	10	5	5	5	10	10	5	14.36	81.86
	Cuk	10	5	6.67	5	5	10	10	7.5	2.5	14.68	76.35
	SEPIC-Zeta	10	5	6.67	5	5	10	10	7.5	2.5	15	76.67
	Cascaded Buck-Boost	15	7.5	10	3.33	3.33	15	6.67	7.5	3.75	15	87.09
	Switched Capacitor	10	10	6.67	3.33	3.33	15	6.67	5	2.5	15	65.84
	Interleaved	10	5	10	3.33	3.33	5	6.67	5	2.5	15	65.84
Insulated	Flyback	10	7.5	10	5	5	10	10	7.5	2.5	13.08	80.58
	Dual H-bridge	10	2.5	3.33	3.33	3.33	10	6.67	2.5	1.25	14.68	57.60
	Dual active bridge	15	2.5	10	1.66	1.66	15	3.33	2.5	1.25	14.84	67.75
	Push-Pull	10	2.5	10	3.33	3.33	10	6.67	5	2.5	13.72	67.06
	Forward	10	2.5	10	5	5	10	10	7.5	2.5	14.04	76.54

The analysis reveals, as shown in Table 4, that isolated structures generally scored lower, with the Dual Half Bridge (DHB) achieving 57.60 % and other structures like Interleaved, Dual Active Bridge (DAB), and Push-Pull topology scoring within the range of 65.84 % to 67.75 %. This outcome is attributable to these structures having more circuit elements, increasing their size, cost, and complexity. Structures such as cuk, sepic-zeta, switched capacitor, and Forward topologies scored between 76.35 % and 77.80 %, indicating significant considerations in terms of dimensions and control akin to those of the Interleaved, DAB, and Push-Pull topologies. Despite this,

the absence of inductors in the switched capacitor topology and the simplicity of the cuk and sepic-zeta topologies yield satisfactory results, albeit with limitations in cost and scalability.

The reversible buck-boost and flyback structures achieved scores of approximately 80.58 % and 81.86 %, respectively. This improvement is attributed to the reduced number of components, which simplifies control and enhances performance.

The cascaded buck-boost structure was awarded the highest score, surpassing the buck-boost and flyback topologies by about 6 %. Despite its increased complexity due to more switches, this topology offers significant advantages, including flexibility in voltage step-up and step-down capabilities in both directions. It is particularly suitable for applications involving batteries from different families and requiring high-density power scalability. Therefore, the cascaded Buck-Boost topology is the most favorable option among the topologies evaluated.

4. RESULTS AND DISCUSSIONS

Four operational scenarios, designed to highlight limitations and distinctions between the Cascaded Buck-Boost and Buck-Boost topologies, are used to assess circuit performance:

- Scenario 1: forward buck mode energy transfer between Lead-Acid and LiFePO4 batteries, charging LiFePO4 with 1A current pulse. Lead-Acid battery SOC exceeds LiFePO4 battery SOC.
- Scenario 2: reverse boost mode energy transfer between Lead-Acid and LiFePO4 batteries, discharging LiFePO4 with -1A current pulse. LiFePO4 battery SOC exceeds Lead-Acid battery SOC.
- Scenario 3: forward buck mode energy transfer between two LiFePO4 batteries charged with a 0.2A current pulse. The First LiFePO4 battery SOC exceeds the second.
- Scenario 4: reverse boost mode energy transfer between two LiFePO4 batteries, discharging with –0.2A current pulse. The second LiFePO4 battery SOC exceeds the first.

Figures 3 to 6 showcase the output current for two different topologies under these scenarios: the cascaded buck-boost converter (IL – in purple) and the buck-boost converter (IL1 – in light blue). Also, Fig. 3 contains details about the current ripple, similar to the other figures. A Lead-Acid battery rated at 14.5 V and an LFP battery rated at 2.5 V were utilized for this analysis.

Given the higher SOC of the Lead-Acid battery relative to the LFP battery, the converters are operated in buck mode, facilitating the charging of the LFP battery with a consistent current of 1A. Notably, both converters regulate the current effectively, with a ripple of less than 5 %. However, it is observable that the stabilization time for the Buck-Boost converter is approximately twice that of the cascaded buck-boost, at 8 ms compared to 4 ms, Fig. 3. Scenario 2, depicted in Fig. 4, involves applying a discharging current of –1A, thereby operating the converters in boost mode, with stabilization times nearly mirroring those observed in the previous scenario.

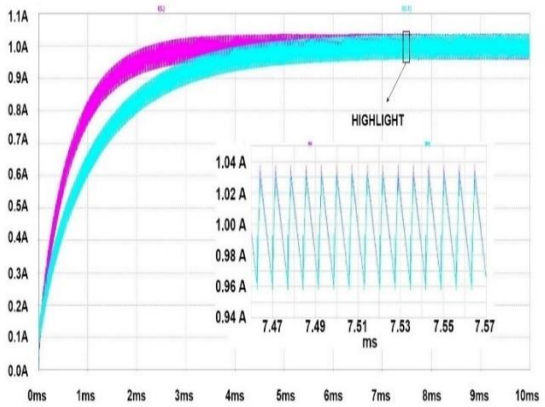

Fig. 3 – Scenario 1: forward buck mode with 1A charging current.

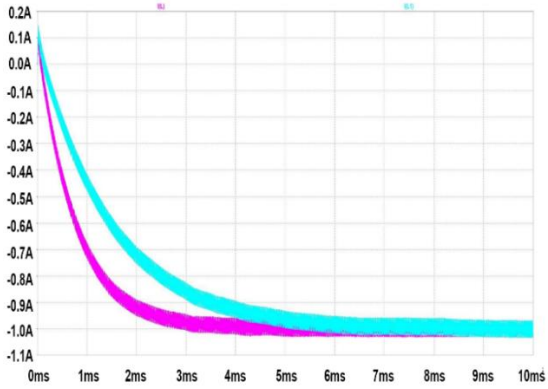

Fig. 4 – Scenario 2: reverse boost mode with -1A discharging current.

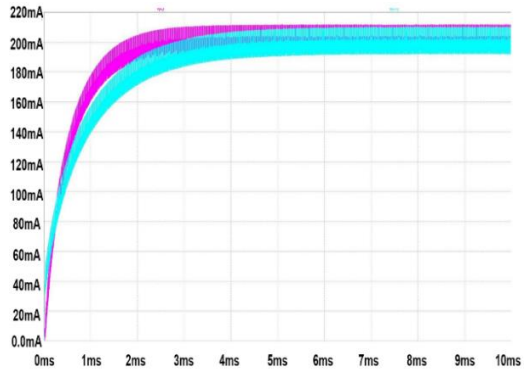

Fig. 5 – Scenario 3: forward buck mode with 0.2A charging current pulse.

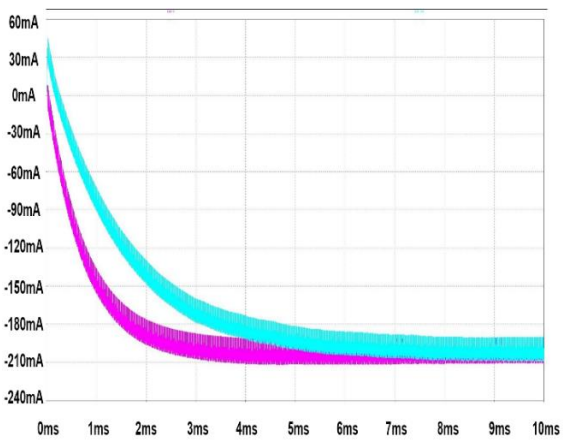

Fig. 6 – Scenario 4: reverse boost mode with discharging current pulse of – 0.2 A.

The outcomes of Scenario 3 are illustrated in Fig. 5, where two LFP batteries with differing SOCs are subjected to a current pulse of 0.2 A.

The battery with the lower SOC is positioned on the output side of the converters, thus operating in buck mode. In this scenario, the current ripple remains under 5 % for both converters, albeit with the buck-boost converter exhibiting a longer stabilization time than the cascaded buck-boost. A prolonged stabilization period is also evident in Scenario 4, as presented in Fig. 6.

These test scenarios effectively elucidate the operational boundaries of the proposed power converters, confirming a maximum output power of 15 W in scenarios 1 and 2. The cascaded buck-boost converter's adaptability is underscored by its broad input and output voltage range across all scenarios, affirming its suitability for multi-technology battery testing.

5. **CONCLUSIONS**

This paper presents a performance evaluation of two optimal bidirectional DC-DC power converters selected through multi-criteria analysis tailored to battery screening systems. Based on the defined criteria, the buck-boost and cascaded buck-boost converters emerged as the most suitable topologies. Circuit design and behavioral analysis were conducted through LTspice simulations.

The buck-boost converter offers advantages in size and cost due to its reduced component count (two power switches and a smaller output filter capacitor). However, its voltage conversion can only achieve step-up in one direction and step-down in the other, necessitating careful battery placement according to state of charge (SOC) and chemistry. Conversely, the cascaded buck-boost topology enables bidirectional voltage step-up/step-down, providing flexibility for integration in multi-chemistry/multi-technology systems. This flexibility allows simultaneous testing of two or more batteries with independent charge/discharge control. Furthermore, simulations demonstrate a significantly faster stabilization time for the Cascaded Buck-Boost topology.

Cascaded buck-boost topology obtained 87.09 points, compared to the buck-boost converter, which has 81.86 points. The difference in points is obtained for power density, which is three times higher, and flexibility. In third place is the flyback converter, which has approximately 81 points, followed by cuk, SEPIC-Zeta, and forward converter, which has around 76 points. The last places are held by the dual active bridge topology, push-pull, switched capacitor, Interleaved, and with the lowest score, dual H-bridge.

Received on 20 March 2023

REFERENCES

1. S. Seba, M. Birane, K. Benmouiza, *A comparative analysis of boost converter topologies for photovoltaic systems using MPPT (P&O) and beta methods under partial shading*, Rev. Roum. Sci. Techn. – Électrotechn. et Énerg., **68**, *4*, pp. 375–380 (2023).
2. J. G. Malar, V. Thiyagarajan, N. B. M. Selvan, M. D. Raj, *Electric vehicle onboard charging via Harris-Hawks optimization-based fractional-order sliding mode controller*, Rev. Roum. Sci. Techn. – Électrotechn. et Énerg., **68**, *1*, pp. 30–35 (2023).
3. J. Li, S. He, Q. Yang, Z. Wei, Y. Li, H. He, *A comprehensive review of second life batteries toward sustainable mechanisms: potential, challenges, and future prospects*, IEEE Trans. Transp. Electrification, **9**, *4*, pp. 4824–4845 (2023).
4. Q. Dong, S. Liang, J. Li, H. C. Kim, W. Shen, T. J. Wallington, *Cost, energy, and carbon footprint benefits of second-life electric vehicle battery use*, iScience, **26**, *7*, p. 107195 (2023).
5. P. Eleftheriadis *et al.*, *Second life batteries: current regulatory framework, evaluation methods, and economic assessment: reuse, refurbish, or recycle*, IEEE Ind. Appl. Mag., **30**, *1*, pp. 46–58, (2024).
6. M. Terkes, A. Demirci, E. Gokalp, *An evaluation of optimal sized second-life electric vehicle batteries improving technical, economic, and environmental effects of hybrid power systems*, Energy Convers. Manag., **291**, p. 117272 (2023).
7. M. S. H. Lipu *et al.*, *A review of state of health and remaining useful life estimation methods for lithium-ion battery in electric vehicles: Challenges and recommendations*, J. Clean. Prod., **205**, pp. 115–133 (2018).
8. E. Martinez-Laserna *et al.*, Battery second life: *Hype, hope or reality? A critical review of the state of the art*, Renew. Sustain. Energy Rev., **93**, pp. 701–718 (2018).
9. T. Bruen, J. Marco, *Modelling and experimental evaluation of parallel connected lithium-ion cells for an electric vehicle battery system*, J. Power Sources, **310**, pp. 91–101, (2016).
10. A. Carloni, F. Baronti, R. Di Rienzo, R. Roncella, R. Saletti, *Open and flexible Li-ion battery tester based on Python language and Raspberry Pi*, Electronics, **7**, *12*, p. 454 (2018).
11. Y. Li, K. Li, Y. Xie, J. Liu, C. Fu, B. Liu, *Optimized charging of lithium-ion battery for electric vehicles: Adaptive multistage constant current–constant voltage charging strategy*, Renew. Energy, **146**, pp. 2688–2699, (2020).
12. A. Al-Haj Hussein, I. Batarseh, *A review of charging algorithms for nickel and lithium battery chargers*, IEEE Trans. Veh. Technol., **60**, *3*, pp. 830–838 (2011).
13. J. Diaz, J. A. Martin-Ramos, A. M. Pernia, F. Nuno, F. F. Linera, *Intelligent and universal fast charger for Ni-Cd and Ni-MH batteries in portable applications*, IEEE Trans. Ind. Electron., **51**, *4*, pp. 857–863 (2004).
14. M. Yilmaz, P. T. Krein, *Review of battery charger topologies, charging power levels, and infrastructure for plug-in electric and hybrid vehicles*, IEEE Trans. Power Electron., **28**, *5*, pp. 2151–2169 (2013).
15. H. A. Serhan, E. M. Ahmed, *Effect of the different charging techniques on battery life-time: Review*, International Conference on Innovative Trends in Computer Engineering (ITCE), Aswan: IEEE, pp. 421–426 (2018).
16. Y. Li, X. Yan, G. Chen, *Design of intelligent accumulator charger for wind power generation system*, Energy Procedia, **17**, pp. 825–833 (2012).
17. M. Şahin, *A comprehensive analysis of weighting and multicriteria methods in the context of sustainable energy*, Int. J. Environ. Sci. Technol., **18**, *6*, pp. 1591–1616 (2021).
18. D. Ravi, S. S. Letha, P. Samuel, B. M. Reddy, *An overview of various DC-DC converter techniques used for fuel cell-based applications*, International Conference on Power Energy, Environment and Intelligent Control (PEEIC), Greater Noida, India, pp. 16–21 (2018).
19. K. Tytelmaier, O. Husev, O. Veligorskyi, R. Yershov, *A review of non-isolated bidirectional dc-dc converters for energy storage systems*, in II International Young Scientists Forum on Applied Physics and Engineering (YSF), Kharkiv, Ukraine, pp. 22–28 (2016).
20. G. Lithesh, B. Krishna, V. Karthikeyan, *Review and comparative study of bi-directional DC-DC converters*, IEEE International Power and Renewable Energy Conference (IPRECON), Kollam, India, pp. 1–6 (2021).
21. D. Ravi, B. Mallikarjuna Reddy, S. S.L, P. Samuel, *Bidirectional DC to DC converters: an overview of various topologies, switching schemes and control techniques*, Int. J. Eng. Technol., **7**, *4.5*, p. 360, (2018).
22. S. Alatai *et al.*, *A review on state-of-the-art power converters: bidirectional, resonant, multilevel converters and their derivatives*, Appl. Sci., **11**, *21*, p. 10172 (2021).
23. M. İnci, M. Büyük, M. H. Demir, G. İlbey, *A review and research on fuel cell electric vehicles: Topologies, power electronic converters, energy management methods, technical challenges, marketing and future aspects*, Renew. Sustain. Energy Rev., **137**, p. 110648 (2021).

24. P. K. Maroti, S. Padmanaban, M. S. Bhaskar, V. K. Ramachandaramurthy, F. Blaabjerg, *The state-of-the-art of power electronics converters configurations in electric vehicle technologies*, Power Electron. Devices Compon., **1**, p. 100001 (2022).
25. K. L. Jorgensen, M. C. Mira, Z. Zhang, M. A. E. Andersen, *Review of high efficiency bidirectional dc-dc topologies with high voltage gain*, 52nd International Universities Power Engineering Conference (UPEC), Heraklion, pp. 1–6 (2017).
26. Ö. Ekin, G. Arena, S. Waczowicz, V. Hagenmeyer, G. De Carne, *Comparison of four-switch buck-boost and dual active bridge converter for DC microgrid applications*, IEEE 13th International Symposium on Power Electronics for Distributed Generation Systems (PEDG), Kiel, Germany, pp. 1–6 (2022).
27. H. Yun, M. Dong, Y. Jian, J. Wan, M. Shen, Y. Wang, *Application of soft-switching technology in four switch buck-boost circuit*, 12th IEEE Conference on Industrial Electronics and Applications (ICIEA), Siem Reap, Cambodia, pp. 1675–1679 (2017).
28. T. H. Van, T. Le Van, T. M. N. Thi, M. Q. Duong, G. N. Sava, *Improving the output of DC-DC converter by phase shift full bridge applied to renewable energy*, Rev. Roum. Sci. Techn. – Électrotechn. et Énerg., **66**, *3*, pp. 175–180 (2021).